Electronic Supplementary Information for:

Robust Electrochemical System for Screening Single Nucleotide Polymorphisms

Experimental Section

Chemicals

Oligonucleotides involved were synthesized by Shanghai Sangon Biological Engineering Technology and Services Co., Ltd (Shanghai, China), and their sequences are listed in Table S1. All the oligonucleotides are dissolved in 50 mM Tris-HCl (pH 7.4) containing 400 mM NaCl prior to use.

*Eco*RI (15 U/μL) accompanied by 10×buffer was obtained from Takara Biotechnology Co., Ltd. (Dalian China). Prior to target assay, 10×buffer was diluted 5-fold with water to prepare the cleavage buffer. Methylene blue solution (25×10^{-6} M) was prepared with 10 mM phosphate buffer solution (0.3 M PBS, pH 7.4) with 0.3 M NaCl.

All other chemicals were of analytical grade and used as received. Deionized and sterilized water (resistance>18 MΩ·cm) was used throughout the experiments.

Preparation of Detection Probe-Functionalized Gold Nanoparticles

Gold nanoparticles (GNPs) were prepared by citrate reduction of $HAuCl_4$ according to the literature method [1]. Prior to modification, GNPs were concentrated via centrifuging 4 mL of stock solution at 15000 rpm and resuspending in 1.5 mL water. Under magnetic stirring, 500 μL of detection probe (371 nM) was gradually injected, and the thiol-gold self-assembly was allowed to proceed for 24 h at room temperature (~ 25℃). Subsequently, 200 μL of 500 mM Tris-HCl (pH 7.4) containing 4 M NaCl was slowly added, and the mixture was stirred for an additional 12 h. The resulting solution was

centrifugated at 14000 rpm to remove the supernatant. The particles were resuspended in 1 mL of water. After being washed two times, the resulting GNPs were redissolved in 2 mL of 50 mM Tris-HCl (pH 7.4) containing 0.3 M NaCl, obtaining the detection probe-functioned GNP solution (called DPGNP).

Fabrication of Interrogating Electrode

Glassy carbon (GC) electrodes were polished with emery paper (# 2000), 0.3- and 0.05-μm alumina slurry and then successively rinsed for 5 min with acetone, ethanol, and distilled water in ultrasonic bath. Subsequently, zirconia nanoparticles (ZrO_2) were electrodeposited onto the cleaned surface of GC electrode according to the literature method [2]. The ZrO_2 modified GC electrode (denoted as ZrGC electrode) was washed with water for the SNP screening.

Apparatus and Electrochemical Measurements

Scanning electron microscopy (SEM) analysis was performed with a JSM-5600LVmicroscope (JEOL Ltd., Japan).

Electrochemical experiments were carried out using CHI 760B electrochemical workstation (Shanghai, China) except for impedance measurements. A normal three-electrode configuration consisting of the bare or modified glassy carbon working electrode, the platinum foil counter electrode and a saturated calomel reference electrode (SCE) was involved. Cyclic voltammetry (CV) measurements were performed in the scan range from -0.2 to +0.6 V at a scan rate of 100 mV/s. Alternating current (AC) voltammetry was conducted at an amplitude of 25 mV, a frequency of 1 Hz, and a sample period of 1.1 s. The peak currents presented in our study were recorded from the automatic reading system. Impedance spectra were collected over a voltage frequency

range of 1 to 100 000 Hz at an initial potential of 240 mV with the AC potential amplitude of ±5 mV. The supporting electrolyte for the AC voltammetric measurements was 10 mM PBS with 0.1 M KCl while AC impedance and cyclic voltammetry were conducted in 10 mM PBS containing 0.1 M KCl and 5 mM $K_3[Fe(CN)_6]/K_4[Fe(CN)_6]$ redox couple.

Electrochemical Screening of Single Nucleotide Polymorphisms

A 6-μL droplet of HP solution (160 nM) was mixed with 3 μL of target DNA of a specific concentration, and the hybridization was kept for 60 min at room temperature. Subsequently, 3 μL of CDNA1 (351 nM) (Complementary DNA sequence 1, of which the italicized and bolded segments are complementary to the italicized segment of hairpin-type probe (HP) and the bolded segment of detection probe, respectively) was injected, followed by incubation for another 60 min, the ratio for HP:target:CDNA were kept at 1:1:1. Then, the cleavage buffer (12 μL) and the endonuclease stock solution (2 μL) were successively added. The cleavage reaction was allowed to occur at 37 ℃ for 120 min. The resulting solution was dropped onto the ZrGC electrode surface to adsorb cleavage products for 120 min. After washing stringently, 20 μL of DPGNP was pipetted onto the resulting electrode surface to amplify the target/HP hybridization event. To obtain a detectable electrochemical signal, the resultant electrode was immersed into the methylene bule solution for 40 min. The modified electrode washed with 50 mM Tris-HCl (pH 7.4) containing 0.4 M NaCl. The peak currents recorded in AC voltammograms were used to evaluate the SNP screening performance of assay platform.

Gel Electrophoresis

The gel electrophoretic analysis was carried out on 3% agarose gels by Gold View

staining, cast and run in 0.5×TBE buffer (4.5 mM Tris, 4.5 mM boric acid, 0.1 mM EDTA, pH 7.9) at room temperature. Electrophoresis was performed at a constant potential of 100 V for 90 min with loading of 8 μL of each sample into the lanes. The resulting gel was excited using a WD-9403F UV device and imaged with a Canon digital camera. A 1-μL droplet of HP solution (2 μM HP) was mixed with 1 μL of target DNA (2 μM T1), and the hybridization was kept for 60 min at room temperature. Subsequently, 1 μL of CDNA1 (2 μM) was added and followed by incubation for another 60 min. Then, the cleavage buffer (3 μL) and the endonuclease stock solution (2 μL) were successively added. The cleavage reaction was allowed to occur at 37 ℃ for 120 min. When performing the control experiments, the corresponding buffers are used instead of the reagent solutions.

Supplementary Figures

Optimization of Restriction Cleavage Site

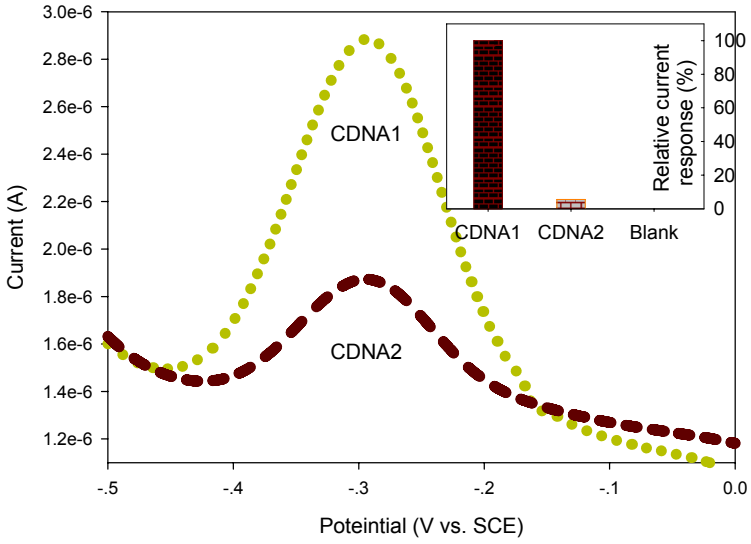

Fig. S1. The dependence of the peak current induced by target DNA on the sequence of CDNA. The concentration of target DNA used is initial concentration 369 nM while the concentrations of CDNA1 and CDNA2 are 351 nM and 383 nM, respectively. Inset: quantitative evaluation of signal transduction capabilities of CDNAs. The relative current response is defined as $(I_{peak}-I_{blank})/(I_{CDNA1}-I_{blank})\times 100\%$. Naturally, the signal intensities observed for CDNA1 in the present and absence of target DNA (blank) are 100% and 0%, respectively.

The incorporation of a binding site for the *Eco*RI restriction enzyme into the oligomers provides a mechanism for transducing target recognition and amplifying current signal. Since *Eco*RI binds only to the double-stranded DNA [3], the most critical issue of the present electrochemical DNA detection system lies in the proper competition between the stem of HP and CDNA/HP duplex. The stable duplex between 5′-terminal single stranded segment of HP and its complementary DNA (CDNA) should be formed only after the stem-loop structure was opened by target DNA. On the other hand, in the absence of target DNA, HP should fold into the hairpin structure due to the favorable formation of the stem hybrid even though the solution contained CDNA, inhibiting the cleavage reaction and subsequent signaling process. For this purpose, with the help of DNA folding software based on the previous works [4,5], two CDNA was designed via controlling the length of complementary segment to HP, and the current responses recorded from the AC voltammograms upon introduction of target DNA were evaluated. As shown in Fig. S1, there is a substantial difference between AC voltammetry collected for CDNA1 and that for CDNA2 even though the higher concentration of CDNA2 was involved, demonstrating the significant difference in the ability to signal the target hybridization event. The relative current response was also used to estimate quantitatively the efficiency of the signal transduction (seen in Fig. S1 Inset). Only a small

electrochemical signal was obtained for the CDNA2 in comparison to that offered by the Blank. Presumably, even in the presence of target DNA, the CDNA2/HP duplex with a short double-stranded region is not stable enough to provide a reliable binding site for the *Eco*RI restriction enzyme. This speculation not only was based on the observation for CDNA2, but also was confirmed by the theoretical value of CDNA2's melting temperature (T_m: ~38 ℃ under given conditions) and the following results. To increase the stability of CDNA/HP duplex and not disturb the target/HP hybridization, CDNA1 was designed by substituting "GG" for "TT" to increase the T_m of CDNA/HP hybrid to ~51 ℃. As expected, in this case, the relative current response was improved by a factor of ~20.

Electrochemical Characterization of Electrochemical Biosensor

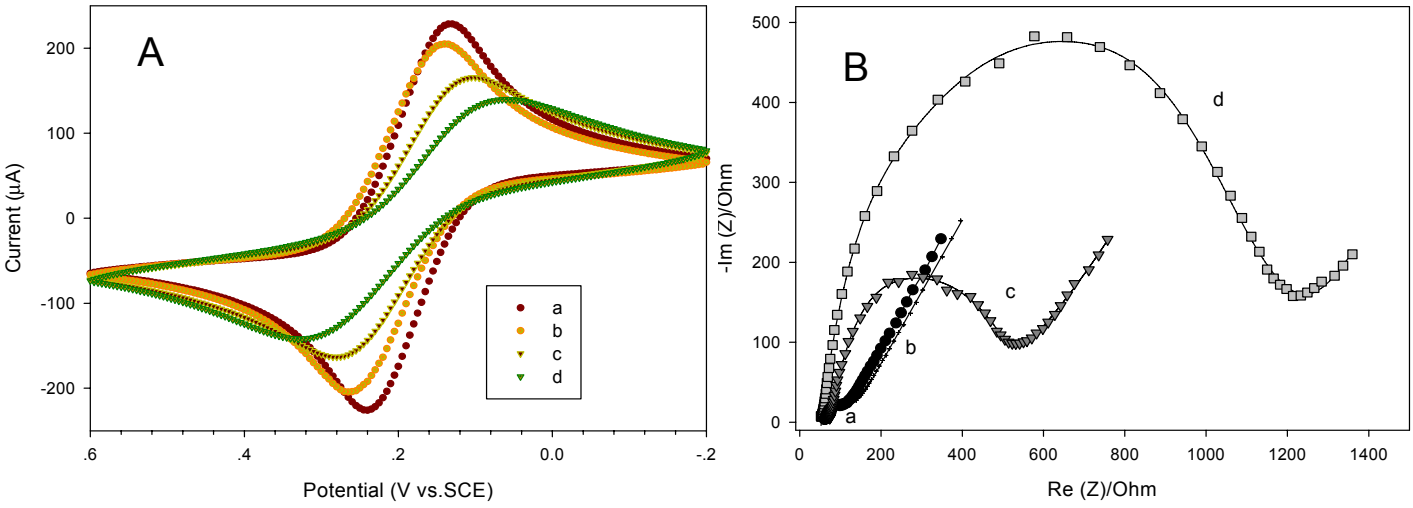

Fig. S2. Cyclic voltammograms (A) and typical Nyquist diagrams (B) obtained for the electrochemical biosensor at different stages of target DNA detection process. (a) Bare GC

electrode; (b) Nano-ZrO_2-modified GC electrode; (c) Cleavage products-attached ZrGC electrode; (d) The same as (c) but with DPGNP amplifiers. The target DNA at initial concentration 369 nM was involved.

Good electrical conductivity is a critical issue to facilitate the electron transfer and to improve the performance of an electrochemical sensor. Thus, the electrical conductivity of the film-modified electrode at different stages during the target DNA analysis was evaluated. As shown in Fig. S2A, the cyclic voltammogram at the bare GC electrode exhibits a pair of reversible redox peaks with very high peak currents (line a); electrodeposition of nano-ZrO_2 film onto the GC electrode results in a slight decrease of the peak currents (line b). Compared with the classical sensing interfaces modified with the self-assembled monolayer of thiol-terminated oligonucleotides regardless of their secondary structure [6,7], the ZrGC electrode displays a much higher rate of electron transfer, favoring the improvement in the analytical performance of DNA detection system. The attachment of cleavage products onto the modified electrode induces an obvious decrease in peak current accompanied by the increase in the peak-to-peak separation (seen in line c). This phenomenon is explained by a fact that the electrostatic repulsion between anionic $[Fe(CN)_6]^{3-/4-}$ and the surface-confined DNA sequences with negative charges retards the interfacial electron-transfer kinetics. Subsequent hybridization of DPGNPs further impedes the interfacial electron transfer (line d) originating from the increase in the surface charge density. Nevertheless, a pair of obvious reversible redox peaks is still observed in comparison to literature observation [6], indicating a desirable electrical conductivity.

As a powerful technique to characterize the interface properties of modified electrodes, electrochemical impedance spectroscopy was also used to elucidate the change in the

interfacial electron transfer feature upon addition of target DNA. Fig. S2B represents Faradaic impedance spectra (presented as Nyquist plot) of the same electrode with different modified surfaces. Only a slight impedance change (line b) is seen after electrochemical deposition of nano-ZrO_2 film, ensuring good electric conductivity for transducing the target recognition into a detectable signal. This observation is consistent with that in cyclic voltammograms of Fig. S2A. As seen in Fig. S2B line c, the attachment of cleavage products onto ZrGC electrode triggers the increase in both imaginary and real parts of the Faradaic impedance from almost zero compared with the insignificant impedance shift induced by the Blank (not shown). Hybridization of DPGNPs to the surface-confined cleavage products increases further the impedance value (line d), indicating a desirable signal amplification. Additionally, we infer that the dissociation of covalently bound cleavage products from the ZrGC electrode does not occur since the electrochemical impedance for the electrode c did not display obvious changes even though the cleavage products-attached surface was washed for longer periods of time and/or under severe conditions (e.g., basic solution). The measured data indicated that the cleavage products and DPGNPs can be successfully immobilized onto the ZrGC electrode, and a good electrical conductivity is preserved even for the DPGNPs-modified electrode compared with literature sensing interface [7]. The proposed electrochemical biosensing system is expected to possess the improved performance for the SNP screening.

Cleavage Product Adsorption Time

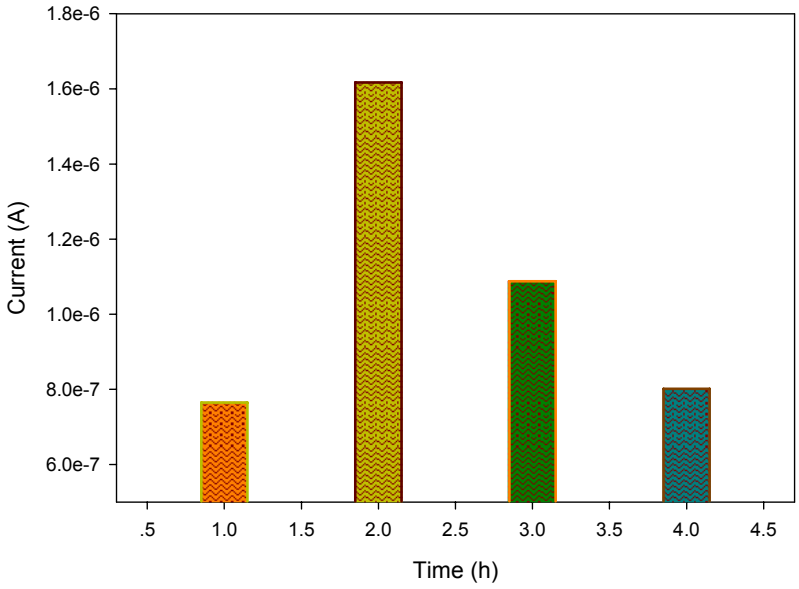

Fig. S3. The effect of incubation time for adsorbing cleavage products onto the ZrGC electrode surface on the analytical performance of sensing system. The target DNA at initial concentration 369 nM was involved. The peak currents upon target DNA were obtained under identical conditions except for the adsorption time of cleavage products.

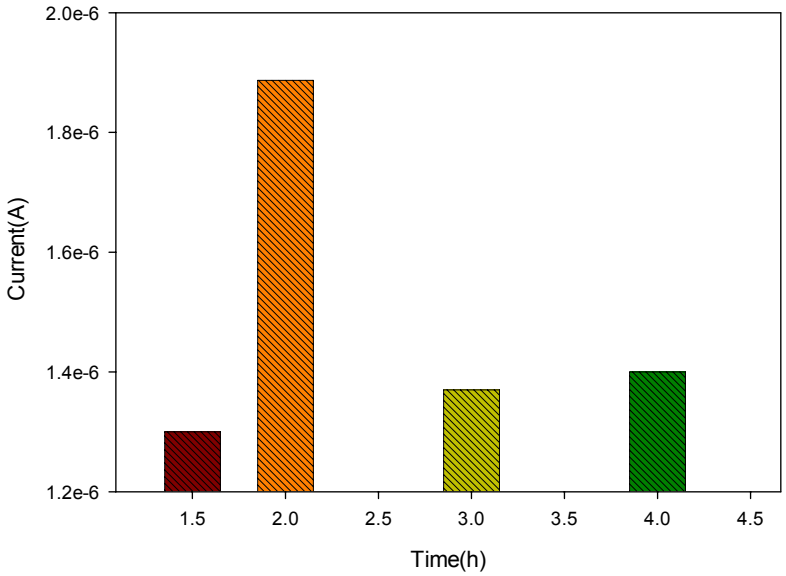

Fig. S4. The effect of incubation time for binding phosphorylated oligonucleotides onto the ZrGC

electrode surface on the analytical performance of the sensing system.

To improve the analytical performance of this DNA detection system, the incubation time for attaching the cleavage products onto the working electrode surface was optimized because it directly determined of the adsorption amount of cleavage products. The dependence of peak current recorded on the adsorption time is afforded in Fig. S3. One can see that a 2-h adsorption time offer a maximal peak current. Unexpectedly, increasing further the incubation time not leads to the increase of peak current but induces a robust diminution. Besides phosphorylated oligonucleotides in the cleavage product solution, there are nonphosphorylaed oligonucleotides and endonucleases. According to literature works [8,9], there is some interaction between ZrO_2 nanomaterials and the biomolecules (including nonphosphorylated oligonucleotides), and this mechanism has been utilized to prepare biosensors. Thus, plausibly, for the longer periods of adsorption time, the interaction between these biomolecules and the surface of ZrGC electrode inhibits the hybridization of DPGNPs with the surface-confined phosphorylated sequences. Additionally, for the terminal phosphorylated oligonucleotides, the anchorage of phosphate backbone onto the electrode surface would change their conformation and in turn leaded to the loss of hybridization ability [10,11]. Naturally, a 2-h period was used for attaching the cleavage products onto the ZrGC electrode surface.

To confirm that the optimum immobilization time is dependent on the terminal phosphorylated oligonucleotides, two 5’ phosphorylated oligonucleotides (P1 and P2 shown in Table S1) with the same sequences as the phosphorylated cleavage products were designed. The kinetic performance of binding the oligonucleotides to the ZrGC modified electrode was investigated in details. Briefly, P1 is mixed with P2. In the

resulting solution, their final concentrations were 250 nM. Subsequently, 20 μL of the mixture was pipetted onto the surface of the ZrGC electrode and was allowed to incubate for different durations. After washing, 20 μL of DPGNPs was dropped onto the electrode surface and hybridization was kept for 2 h. Then, the accumulation of methylene blue and the current measurement of the resulting ZrGC electrode were carried out under the same conditions as those involved for detecting cleavage products. The results are shown in Fig. S4. As can be seen, the similar trend is observed as compared with the results depicted in Fig. S3, demonstrating the reasonability of the selected incubation time and the corresponding explanation.

Feasibility of the Sensing Scheme for Other Target DNA

In order to investigate the universal applicability of the sensing method, another hairpin probe and corresponding oligonucleotide strands are designed and the detections were carried out according to the method described in the section of "Experimental Secrion". Their sequences are shown below:

HP2: 5'-TTC GCC GGC AGT CAG TGT GGA AAA TCT CTA GC GCC GGC *GAA TTC* **TTA AAA CCT CTT GAT**-3' AGAAGATATTTGGAATAACATGACCTGGATGCA

T5: 5'-GC TAG AGA TTT TCC ACA CTG ACT-3'

T6: 5'-GC AAG AGA TTT TCC ACA CTG ACT-3'

T7: 5'-GC TAG AGA TTT TCC ACA CTG AGT-3'

T8: 5'-GC TAG AGA TTT TGC ACA CTG ACT-3'

The loop region of HP3 is different from HP designed in the manuscript, while the other segments are the same. The target sequence T5, which is related to HIV-1, is

complementary to the loop region as seen in HP2. The mutant bases in T6, T7 and T8 are underlined. The experimental results are shown in Fig. S5. Obviously, the single-base mismatched sequences, T6-T8, can be discriminated from the complementary target, T5, validating the universality of the proposed sensing strategy.

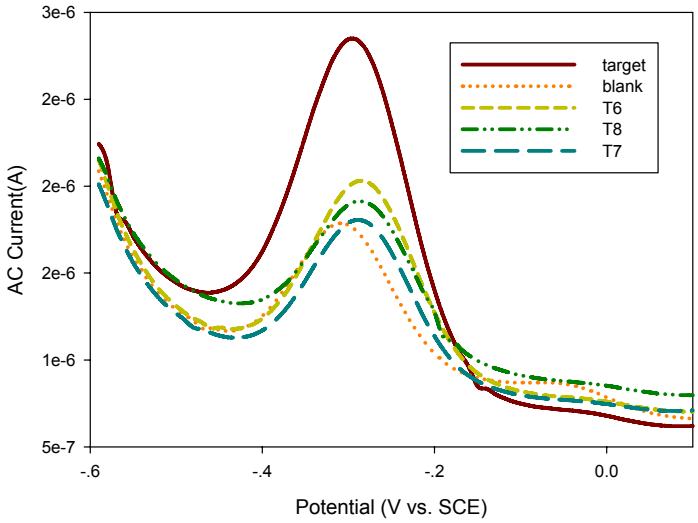

Fig. S5. Analytical performance for different target sequences when HP1 system is used. The target DNA, T5, T6, T7, T8 and CDNA1 at initial concentration 400 nM were involved, and the concentration of HP2 used was concentration 200 nM. The ratio for HP:target:CDNA1 was kept at 1:1:1.

Electrophoresis Characterization

The first four lanes (lane 1, 2, 3 and 4) showed HP/T1/CDNA1-probe/*Eco*RI mixture, HP/CDNA1-probe/*Eco*RI mixture, HP/T1/CDNA1-probe mixture, HP/CDNA1-probe mixture, respectively. A migration band appears in lane 4 due to the stem helix of the hairpin-probe (HP). The endonuclease stock solution was added, the band had no substantial change (lane 2) , because HP fold into the hairpin structure due to the favorable formation of the stem hybrid even though the solution contained CDNA1, inhibiting the cleavage reaction. However, the migration band was retarded when incubated with the target (lane 3) compared to HP/CDNA1-probe (lane 4) , indicating the

existence of the HP/T1/CDNA1 complexes. EcoRI can catalyze cleavage reaction of the HP/T1/CDNA1-probe mixture, generating cleavage products. Thus, addition of endonuclease stock solution displayed another notable migration band in a gel (lane 1).

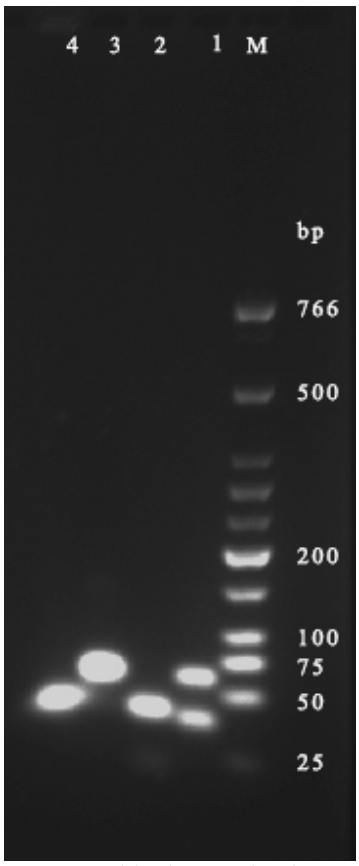

Fig. S6.Gold view stained agarose gel (3%) electrophoresis in 0.5×TBE for 1.5 h. Lane 1: HP /T1/CDNA1-probe/*Eco*RI mixture, Lane 2: HP/CDNA1-probe/*Eco*RI mixture, Lane 3: HP /T1/CDNA1-probe mixture, Lane 4: HP/CDNA1-probe mixture, Lane M: DNA ladders.

Performance Comparison and Intrinsic Feature

To demonstrate unequivocally the capability of the proposed sensing platform to profile SNP in target DNA as well as the distinct advantages, we provided the direct comparison between our results and impressive electrochemical screening systems [12-16] in terms of throughput, speed of sensor preparation, cost effectiveness, assay specificity, sensitivity and so on (shown in table S2). As indicated in literature works [12-16], DNA probes

must be coupled to functional groups in order to prepare the electrochemical sensing interface and/or transducer hybridization event that is time-consuming, expensive, and laborious. By contrast, our label-free SNP profiling scheme does not require any chemical modification of DNA sequences except for the detection probe that is not directly related to the target sequence and can be shared by various recognition probes when different target DNAs are involved, economizing the detection cost and saving the time for synthesizing DNA probes. The literature studies [12-14] investigate the ability of sensors to discriminate the target with single-nucleotide polymorphism (SNP) in the middle of target DNA regardless of whether targets with two- or more-mismatched bases are involved. The discrimination factor is not more than 10 and decreases with the decrease of target concentration [12]. Nevertheless, the identification of SNP close to the end of target DNA is not presented in these works [12-14] because it is possibly not easy to conduct. Although the single-base mismatch close to the 5′ terminus of target DNA can be identified utilizing another screening protocol [15], the discrimination factor is only 1.6. Even if substituting poly(T) system with poly(A) sensor, the single-base mismatch discrimination ability increases to 3 but at the cost of decreased signal gain. Moreover, the assay sensitivity reported by these works [12-16] ranges from 5 nM to 10 fM. Additionally, the preparation of electrochemical sensor [13-16] generally involves several steps and requires a long time (varying from several h to several days). In sharp contrast, the proposed sensing scheme can exhibit an improved SNP screening performance. As shown in Right inset of text Fig. 3, not only can the SNP in the middle of target DNA (namely, T4) be easily distinguished from the complementary target DNA, but also the corresponding peak current exhibits an insignificant difference from that of

the Blank. The discrimination factors for the single-base mismatch at the 5′ terminus and at the 3′ terminus is about 100 and 1.6, respectively. Notably, the screening system retains its excellent discrimination ability even in the presence of high concentration of mismatched target. For example, a discrimination factor is 10.7 for 3.69 fM T1/375 nM T4 sample and 5.1 for 3.69 fM T1/361 nM T2 sample. Seeing form another angle, we can detect the complementary target DNA at 3.69 fM, indicating an assay sensitivity of the femtomolar level. Moreover, preparing signaling interface involves only one step, the electrdeposition of zirconia nanoparticles, and only needs about 50 min. The introduction of homogeneous target recognition into an interfacial signal transduction can make the technique automated, reproducible, and accomplished with minimal working steps. The homogeneous target recognition might be implemented in a parallel or high-throughput manner and the ZrO_2-based interfacial transduction can be adapted to microarray [17-19] that have became an important tool for high throughput analysis of biological systems [14,20]. This could further save the assay time and make high-throughput SNP detection feasible. Additionally, in our sensing scheme, the competitive reaction between the stem of HP and CDNA/HP duplex is designed. Because the hybridized fragments involved are all composed of common Watson–Crick base pairs, the CDNA/HP duplex is opened when the double-stranded stem of HP is disassociated by the nonspecific binding of interferents (e.g., proteins [21]), inhibiting the subsequent cleavage process. Consequently, not only can the Blank but also interferents not produce a false-positive signal as indicated in literature report [21] where only a hairpin-type probe is employed.

Essentially, a designed signaling mechanism determines the analytical performance. The impressive sensing capability of the proposed strategy should be attributed to its

intrinsic feature desirable for applications in typing SNPs, including the following: 1) both the attachment of phosphorylated DNAs and subsequent hybridization with DPGNPs are triggered by the specific target DNA binding (hybridization) without any surface-prehybridized oligonucleotides that might compromise the detection sensitivity [22,23]. This new sensing design would pave the way for generation of an electrochemical signal from scratch upon raising the concentration of target DNA. This not only gives a signal-on response but also avoids the effect of the nonspecific signal, contributing to the improving the performance of DNA biosensors; 2) The digestion of double-stranded fragment by *Eco*RI restriction enzyme [3], the interaction between ZrO_2 nanomaterials and 5′-phosphorylated oligonucleotides [17-19] and the hybridization of hairpin-type probes with their target DNAs [24,25] have proved to exhibit extremely high specificity. Moreover, the ZrO_2 surface-confined oligonucleotides can preserve the ability to hybridize with their complements [17]. Based on the combination of the several elements, the present DNA biosensor naturally has an excellent differentiation ability even for single mismatches; 3) Each target binding event can generate two cleavage products, each cleavage product can "capture" more than one detection probe via being mediated by GNPs and each detection probe can adsorb more than one methylene blue. Especially in the presence of a very small amount of target DNA, this signal amplification scheme is crucial in screening DNA sequences. An elegant cascaded amplification makes this sensing scheme possess advantages for the detection of SNPs over the traditional analytical protocol where a one-to-one correspondence between the target species and signal reporters [26]. Additionally, a good electric conductivity retained after electrodepositon of ZrO_2 onto the GC electrode facilitates the interfacial

electron transfer between redox probes and the electrode surface. Such features make this biosensing system an candidate for the identification and characterization of gene mutations; 4) Oligonucleotides involved do not require any chemical modification except the detection probe, retaining their native bioactivity; 5) The combination of homogeneous target recognition and interfacial transduction circumvents biochemical recognition reactions on the electrode interface. This resulting screening scheme ensures the high efficiency of reactions involved and a high fidelity of sequence discrimination of target oligonucleotides. These advantages endow the developed screening strategy not only with additional design flexibility but also with advantages for the development and application of promising biosensors. Briefly, the improved single-base discrimination capability should be attributed to the synergistic effect of the specific affinity of zirconia for phosphate group, the selective binding of hairpin-type probe to its target strand, the restriction cleavage of DNA hybrid by endonuclease and the DPGNP-based enhanced signaling scheme. The proposed electrochemical platform displayed a distinctive signaling mechanism compared with the conventional sensing systems and provided a new concept in the development of sensitive SNP analysis.

Notes and references

1 Yin, X.-B.; Qi, B.; Sun, X.; Yang, X.; Wang, E. *Anal. Chem*., 2005, **77**, 3525.

2 Liu, G. D.; Lin, Y. H. *Anal. Chem*., 2005, **77**, 5894.

3 Kumke, M. U.; Li, G.; McGown, L. B. *Anal. Chem*., 1995, **67**, 3945.

4 SantaLucia, J. *Proc. Natl. Acad. Sci. U.S.A*., 1998, **95,** 1460.

5 Zuker M. *Nucleic Acids Res*., 2003, **31**, 3406.

6 Cheng, A. K. H.; Ge, B.; Yu, H.-Z. *Anal. Chem*., 2007, **79**, 5158.

7 Steichen, M.; Brouette, N.; Buess-Herman, C.; Fragneto, G.; Sferrazza, M. *Langmuir*, 2009, **25**, 4162.

8 Liu, S. Q.; Dai, Z. H.; Chen, H. Y.; Ju, H. X. *Biosens. Bioelectron*., 2004, **19**, 963.

9 Zhang, W.; Yang, T.; Jiang, C.; Jiao, K. *Colloid. Surface. B*, 2004, **36**, 155.

10 Zhao, W. T.; Lee, T. M. H.; Leung, S. S. Y.; Hsing, I. M. *Langmuir*, 2007, **23**, 7143.

11 Liu, H.; Fu, Z. F.; Yang, Z. J.; Yan, F.; Ju, H. X. *Anal. Chem*., 2008, **80**, 5654.

12 Huang, J. T.; Minghsun, L.; Knight, D. L.; Grody, W. W.; Miller, F. J.; Ho, C. M. *Nucleic Acids Res*., 2002, **30**, e55.

13 Xiao, Y;. Lou, X.; Uzawa, T.; Plakos, K. J. I.; Plaxco, K. W.; Soh. H. T. *J. AM. CHEM. SOC*., 2009, **131**, 15311.

14 Li, X.; Lee, J. S.; Kraatz, H.-B. *Anal. Chem*., 2006, **78**, 6096.

15 Cash, K. J.; Heeger, A. J.; Plaxco, K. W.; Xiao, Y. *Anal. Chem*., 2009, **81**, 656.

16 Xiao, Y.; Qu, X.; Plaxco, K. W.; Heeger, A. J. *J. Am. Chem. Soc*., 2007, **129**, 11896.

17 Nonglaton, G.; Benitez, I. O.; Guisle, I.; Pipelier, M.; Leger, J.; Dubreuil, D.; Tellier, C.; Talham, D. R.; Bujoli, B. *J. Am. Chem. Soc*., 2004, **126**, 1497.

18 Lane, S. M.; Monot, J.; Petit, M.; Tellier, C.; Bujoli, B.; Talham, D. R. *Langmuir*, 2008, **24**, 7394.

19 Monot, J.; Petit, M.; Lane, S.; Guisle, I.; Leger, J.; Tellier, C.; Talham, D. R.; Bujoli, B. *J. Am. Chem Soc*., 2008, **130**, 6243.

20 Harper, J. C.; Polsky, R.; Wheeler, D. R.; Dirk, S. M.; Brozik, S. M. *Langmuir*, 2007, **23**, 8285.

21 Wang, L.; Yang, C.; Medley, C.; Benner, S.; Tan, W. *J. Am. Chem. Soc*., 2005, **127**, 15664.

22 Xiao, Y.; Qu, X.; Plaxco, K. W.; Heeger, A. J. *J. Am. Chem. Soc*., 2007, **129**, 11896.

23 Zhang, W.; Yang, T.; Jiang, C.; Jiao, K. *Appl. Surf. Sci*., 2008, **254**, 4750.

24 Dubertret, B.; Calame, M.; Libchaber, A. J. *Nat Biotechnol*., 2001, **19**, 365.

25 Designing Molecular Beacons, Office of Technology Transfer, Public Health Research Institute, 225 Warren Street, Newark, New Jersey 07103, USA. www.molecular-beacons.org

26 Nakayama, M.; Ihara, T.; Nakano, K.; Maeda, M. *Talanta*, 2002, **56**, 857.

Table S1. The sequences of oligonucleotides[a] involved in the present work.

Note	DNA Sequence
HP：	5’-TTC GCC GGC CCT CAA ATC AAT CCG CCT GCC AAC G*CC GGC GAA TTC* **TTA AAA CCT CTT GAT-3’**
CDNA1：	5’-*GAA TTC GCC GG* **TTA AAA CCT CTT GAT**-3’
CDNA2：	5’- *GAA TTC GCC* **TTA AAA CCT CTT GAT**- 3’
Detection probe:	5’-SH-TCA CCC ACG **ATC AAG AGG TTT TAA**-3’
Perfectly-matched target (T1):	5’-GTT GGC AGG CGG ATT GAT TTG AGG-3’
Single-base mismatched target (T2):	5’-GAT GGC AGG CGG ATT GAT TTG AGG-3’
Single-base mismatched target (T3):	5’-GTT GGC AGG CGG ATT GAT TTG ACG-3’
Single-base mismatched target (T4):	5’-GTT GGC AGG CGC ATT GAT TTG AGG-3’
P1	:5’-$(PO_4)^{3-}$-AATTC**TTAAAACCTCTTGAT**-3’
P2	:5’-$(PO_4)^{3-}$-AATTCGCC**TTAAAACCTCTTGAT**-3’

[a]All the oligonucleotides are dissolved in 5.0 mM Tris-HCl (pH 7.4) containing 40 mM NaCl. Hairpin-type probe (HP) can fold into a hairpin structure due to the hybridization between two regions with gray background, forming a nine-base stem and leaving a single-stranded segment at the 3′ end. In the presence of target, the italicized segment of CDNA1 or CDNA2 is able to hybridize to HP’s italicized one whose part bases are shared with the stem, creating the *Eco*RI recognition site as demonstrated in the square of Scheme 1A. Unless otherwise stated, CDNA1 rather than DNA2 was used throughout. The detection probe is modified with a 3′-alkanethiol, and its bolded segment is complementary to the bolded sequence of CDNA1, CDNA2 or HP. Perfectly matched target (T1) is designed to hybridize to the 24-base loop portion of the HP. The single

mismatched base in T1, T2 or T3 is underlined.

Table S2. Comparison of Analytical Performance of Various Electrochemical Methods for profiling SNPs.

Electrochemical SNP profiling scheme	Requirement for chemical modification of recognition probe	Assay specificity (discrimination factor: match-to-mismatch signal ratio)	Assay sensitivity	Time for preparing signaling surface	Homogeneous recognition reaction	False positive signal	Throughput SNP analysis
Hairpin-forming probe [12]	Yes	7.2 at 10 nM About 2 at 0.1 nM	0.01 pM	Disposable commercial sensor	Non	—	—
Triple-stem DNA probe[13]	Yes	8.1 at 64 nM	5 nM	More than 21 h	Non	No	—
Recognition probe-modified microelectrode array [14]	Yes	More than 9.6 as indicated in literature table 2	10 fM	5 days	Non	—	Yes
Pseudoknot-based electrochemical sensor [15,16]	Yes	[a]1.6 at 100 nM	2 nM [16]	More than 20 h	Non	More than 50%	—
The present screening scheme	No	3.69 fM	3.69 fM	About 50 min	Yes	No	Yes

[a] In this work, the single-base mismatch is close to the 5′ terminus. When substituting poly(T) system with poly(A) sensor, the single-base mismatch discrimination factor increases to 3 but at the cost of decreased signal gain.